ACCOUNTS
of chemical research

Lipid-Shelled Vehicles: Engineering for Ultrasound Molecular Imaging and Drug Delivery

KATHERINE W. FERRARA,* MARK A. BORDEN, AND HUA ZHANG

Department of Biomedical Engineering, 451 Health Sciences Drive, University of California, Davis, California 95616

RECEIVED ON OCTOBER 22, 2008

CONSPECTUS

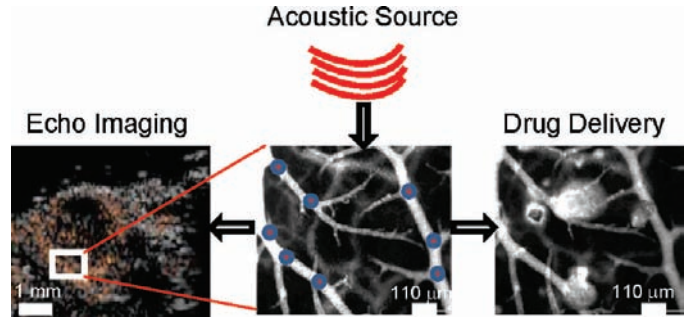

Ultrasound pressure waves can map the location of lipid-stabilized gas microbubbles after their intravenous administration in the body, facilitating an estimate of vascular density and microvascular flow rate. Microbubbles are currently approved by the Food and Drug Administration as ultrasound contrast agents for visualizing opacification of the left ventricle in echocardiography. However, the interaction of ultrasound waves with intravenously-injected lipid-shelled particles, including both liposomes and microbubbles, is a far richer field. Particles can be designed for molecular imaging and loaded with drugs or genes; the mechanical and thermal properties of ultrasound can then effect localized drug release.

In this Account, we provide an overview of the engineering of lipid-shelled microbubbles (typical diameter 1000−10 000 nm) and liposomes (typical diameter 65−120 nm) for ultrasound-based applications in molecular imaging and drug delivery. The chemistries of the shell and core can be optimized to enhance stability, circulation persistence, drug loading and release, targeting to and fusion with the cell membrane, and therapeutic biological effects. To assess the biodistribution and pharmacokinetics of these particles, we incorporated positron emission tomography (PET) radioisotopes on the shell. The radionuclide ^{18}F (half-life ~2 h) was covalently coupled to a dipalmitoyl lipid, followed by integration of the labeled lipid into the shell, facilitating short-term analysis of particle pharmacokinetics and metabolism of the lipid molecule. Alternately, labeling a formed particle with ^{64}Cu (half-life 12.7 h), after prior covalent incorporation of a copper-chelating moiety onto the lipid shell, permits pharmacokinetic study of particles over several days.

Stability and persistence in circulation of both liposomes and microbubbles are enhanced by long acyl chains and a poly(ethylene glycol) coating. Vascular targeting has been demonstrated with both nano- and microdiameter particles. Targeting affinity of the microbubble can be modulated by burying the ligand within a polymer brush layer; the application of ultrasound then reveals the ligand, enabling specific targeting of only the insonified region.

Microbubbles and liposomes require different strategies for both drug loading and release. Microbubble loading is inhibited by the gas core and enhanced by layer-by-layer construction or conjugation of drug-entrapped particles to the surface. Liposome loading is typically internal and is enhanced by drug-specific loading techniques. Drug release from a microbubble results from the oscillation of the gas core diameter produced by the sound wave, whereas that from a liposome is enhanced by heat produced from the local absorption of acoustic energy within the tissue microenvironment. Biological effects induced by ultrasound, such as changes in cell membrane and vascular permeability, can enhance drug delivery. In particular, as microbubbles oscillate near a vessel wall, shock waves or liquid jets enhance drug transport. Mild heating induced by ultrasound, either before or after injection of the drug, facilitates the transport of liposomes from blood vessels to the tissue interstitium, thus increasing drug accumulation in the target region.

Lipid-shelled vehicles offer many opportunities for chemists and engineers; ultrasound-based applications beyond the few currently in common use will undoubtedly soon multiply as molecular construction techniques are further refined.

Published on the Web 06/25/2009 www.pubs.acs.org/acr
10.1021/ar8002442 CCC: $71.50

Introduction

Ultrasound has unique and important opportunities to enhance molecular imaging and drug delivery. The interaction of sound waves with stabilized gas bubbles creates echoes from which images are created. Sound waves can also release encapsulated drugs from both microbubbles and liposomes and enhance transmembrane and extravascular drug transport. This Account focuses on the engineering of lipid-shelled vehicles and their application in ultrasound-mediated molecular imaging and ultrasound-enhanced drug delivery; an overview of these applications is provided in Table 1.

A microbubble is defined here as a gas particle of less than 10 μm in diameter dispersed in aqueous media and used as an intravascular contrast agent for ultrasound imaging. In addition to providing stability by inhibiting dissolution and coalescence, the lipid shell imparts a barrier between the gas and water to reduce thrombogenic effects.[1] The lipidic barrier therefore provides stability and prevents embolism when microbubbles are injected *in vivo*.

Microbubbles produce very strong echoes when driven by ultrasound at a frequency near resonance.[2] As a result, they have found several uses in medical applications, most notably those that exploit their size oscillation when pulsed by ultrasound. Ultrasound imaging applications include detection of heart abnormalities, quantification of reperfusion of the myocardium, and the detection of atherosclerosis.[3] In molecular imaging applications, microbubbles are targeted to luminally-expressed vascular receptors using ligands attached to the shell, where the specific receptors are upregulated in cancer or cardiovascular disease.

Alternatively, liposomes are infrequently described as contrast agents for ultrasound imaging; rather, they are important to consider as drug delivery vehicles, which may accumulate and release their cargo in a target region as a result of local heating by ultrasound or by other means.[4,5] For example, stable long-circulating liposomes containing doxorubicin reduce drug-related toxicity, and liposome formulations where doxorubicin can be locally released by heat are now in clinical trials.[6] Engineering of the liposome for such applications requires efficient drug loading, stability during circulation, and efficient release of the cargo upon insonation/heating.[7] While liposomes have been studied for many years, the combination of heat and drug administration is receiving increased attention due to clinical combinations of radiofrequency ablation and liposomes and the substantial improvements in multimodal technologies.[8] For example, combinations of magnetic resonance imaging and focused ultrasound now can control hyperthermia with spatial resolution on the order of millimeters and temperature accuracy on the order of 1 °C.[9] Clinically-relevant liposomes and microbubbles typically include phospholipids with thermotropic phase transitions that change from a well-ordered gel phase to a less ordered liquid crystalline state. Liposomes are more permeable when their temperature is above the phase transition for the specific lipid formulation, with commercially-available phospholipid molecules demonstrating phase transition temperatures above and below body temperature (Figure 1a).

Microbubbles and liposomes may at first appear to be remarkably different in composition when an internal gas phase is compared to an internal aqueous phase (Figure 1b–d). The microbubble shell is a highly condensed monolayer at the gas/liquid interface, while the liposome membrane is an enclosed, free-standing bilayer. These differences pro-

TABLE 1. Overview of This Account

Methods to enhance:	microbubble	liposome	ultrasound field
stability and circulation persistence of the particle	long acyl chain, low incidence of defects, PEG coating (5–9%), low diffusivity gas[1–3]	long acyl chain, low incidence of defects, PEG coating (3–5%),[4] size, shape,cholesterol incorporation[5]	N/A
ultrasound imaging	diameter chosen to allow resonant oscillation at sound wave frequency[6]	gas entrapment within the bilayer	sound wave pulse sequences are designed with alternating phase, variation in amplitude[6]
receptor targeting and membrane fusion	small diameter, irregular shape (partially deflated or long lipid tails), addition of liposomes to shell exterior, presence of multiple targeting ligands[7–9]	small diameter, dense targeting ligands[5,10]	ultrasound-enhanced targeting results from long, low amplitude pulses at the resonance frequency to deflect microbubbles to the vessel wall[11] or sound-mediated exposure of a buried ligand[12,13]
drug loading and release	layer by layer construction, conjugation of particles to the surface, short acyl chains[7,11,14]	low cholesterol incorporation, short or single acyl chain incorporation[15–17]	ultrasound-enhanced drug release typically results from size oscillation for the microbubble[6] and local heating for the liposome[15]
efficacy based on changes to the biological environment	shock waves or liquid jets produced by oscillating bubbles with a large diameter or high local concentration[6]	addition of drugs or sonosensitizer[18]	the sound field alone can enhance transport[18]

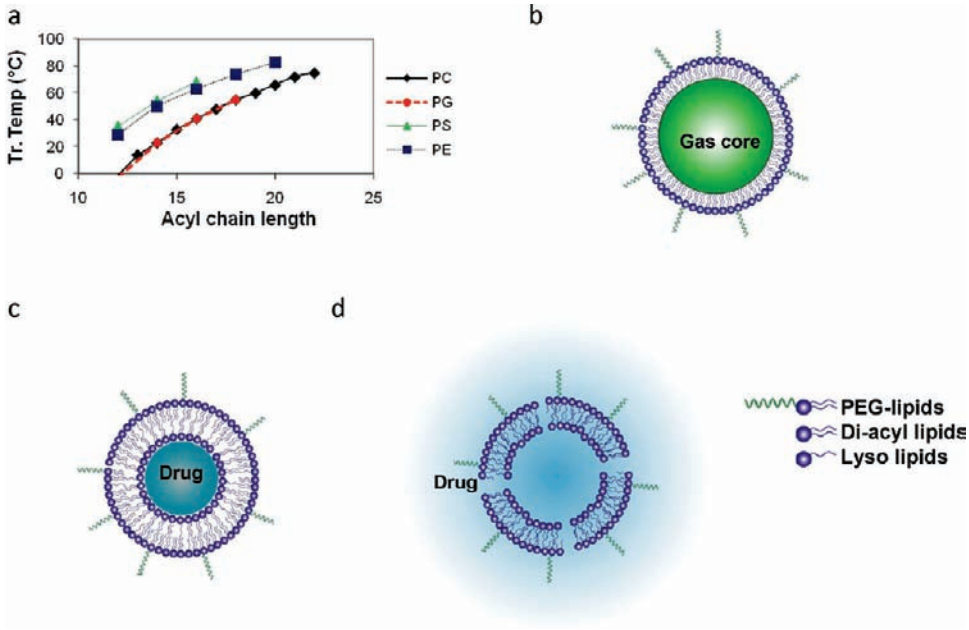

FIGURE 1. Overview of vehicles and lipid components, and biodistribution: (a) phase transition temperature as a function of acyl chain length for four lipid head groups—phosphatidylcholine (PC), phosphatidylserine (PS), phosphatidylglycerol (PG), and phosphotidylethanolamine (PE); (b–d) cartoon representations (not drawn to scale) of microbubbles (b), temperature-sensitive liposomes below their transition temperature (c), and temperature-sensitive liposomes above their transition temperature (d). Typical microbubble and liposome diameters are 1–10 μm and 65–120 nm. Phase transition temperatures near 40 °C are typically chosen for temperature-sensitive vehicles.

vide a broad range of behaviors that can be exploited for ultrasound applications. Many of the key properties, such as stability, circulation persistence, drug loading and release, and ultrasound-mediated bioeffects are highly dependent on the lipid membrane. Because composition is analogous in many situations, and the membrane properties are characterized by the underlying intermolecular forces and packing constraints of the lipid constituents, there are several themes in lipid membrane design that apply to both particle systems.

One ultimately seeks to improve the ultrasound-mediated behavior of injected lipid particles, such as their stability, immunogenicity, targeting efficiency, potential for imaging, payload capacity, and drug release profile. The *in vivo* performance of a lipid particle depends on properties of the protective membrane, such as the surface tension, viscoelasticity, solute permeability, charge density, ligand density and availability, and lipid-shedding behavior. These properties can be tuned through composition, microstructure, architecture, and construction.

Properties of Microbubbles

The typical dose of microbubbles for a human undergoing an echocardiographic evaluation (FDA-approved procedure) is approximately 10^9–10^{10} microbubbles given for a 1–2 mL bolus intravenous injection. The microbubble must be smaller than 10 μm in diameter in order to pass through the lung capillaries. Resonance frequency is strongly dependent on microbubble diameter, with smaller microbubbles resonating at higher frequencies. For a given acoustic frequency, the radial strain and echo strength are strongly dependent on the microbubble size. Therefore, optimization of ultrasound–microbubble interactions for a specific ultrasound frequency requires a narrow size distribution.

The shell of a resting microbubble must be able to compress to a metastable state in which the Laplace overpressure inside the microbubble is essentially zero in order to prevent microbubble dissolution (Figure 2). The lipid monolayer must therefore be highly cohesive and insoluble.[10,11] The ability of the shell to expand during rarefaction and compact during compression of the ultrasonic wave is strongly coupled to the acoustic response of the microbubble. For imaging purposes, where the loudest backscattered echo is desired, the shell should have a high compliance during insonification. A compliant shell also should remain associated with the gas core during oscillation and should restabilize the gas core following oscillation. Lipids appear to be an ideal bioinspired material for achieving these criteria.

The gas core of the microbubble is not only much less dense than water, providing a significant acoustic impedance mismatch, but more importantly it is compressible and can

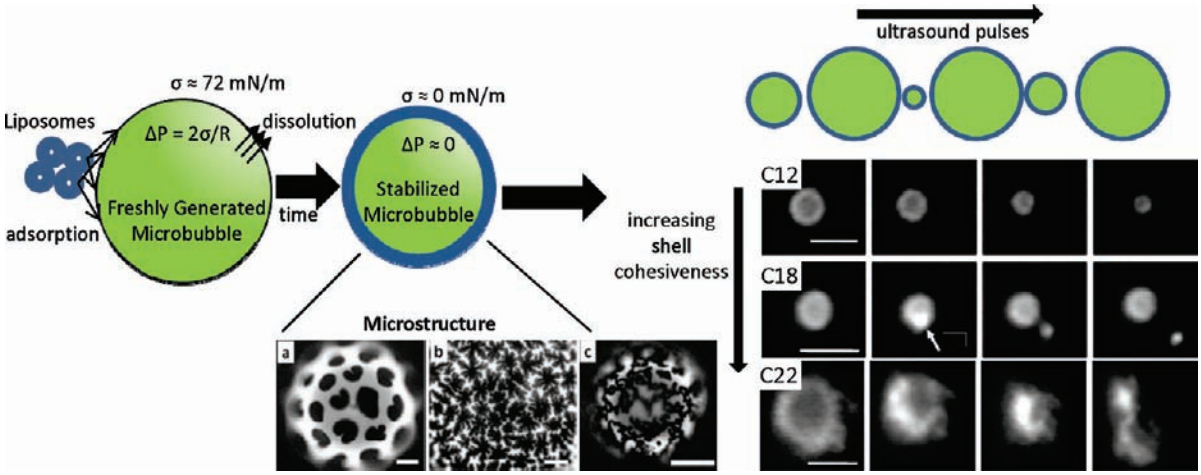

FIGURE 2. Synthesis and stability of microbubbles. Mechanical agitation of liposomes in an aqueous environment results in lipid-coated microbubbles. If the microbubble shell is cooled slowly, domains of lipid components form. On the left, various microstructures are shown, reproduced with permission from ref 23 (Copyright 2004 Elsevier), including (a) large domains after slow cooling, (b) snowflake domains after rapid cooling, and (c) network domains (scale bars are 20 μm). On the right, microbubbles with varying acyl chain length are shown before and after a sequence of ultrasound pulses; microbubbles expel a small volume of gas and lipid with each pulse, reproduced with permission from ref 24 (Copyright 2005 IEEE). After insonation, C_{12} decreases in diameter but exhibits no optically-discernible shed particles, C_{18} sheds a small bud, and C_{22} accumulates lipid that remains attached to the monolayer shell (scale bars are 5 μm). For C_{22}, increasing the acyl chain length increases the cohesiveness of the microbubble shell, and as a result excess lipid remains bound to the smaller bubble after insonation.

therefore expand and shrink with the passage of an acoustic wave. This yields a strong scattered signal in response to an ultrasound wave (known as high "echogenicity"). Liquid and solid particles are relatively incompressible and therefore not as echogenic as microbubbles.

Properties of Liposomes

The typical liposomal drug carrier has a diameter of 65−120 nm, with the small diameter facilitating extravasation through leaky blood vessels and fusion with cellular membranes.[5] Increasing acyl chain length enhances stability in plasma. With the incorporation of long acyl chains and, in some cases, cholesterol, long circulation times and stable drug incorporation are achieved. The typical dose of therapeutic liposomes is dependent on the pathology and encapsulated drug. The most heavily studied particle is liposomally-encapsulated doxorubicin, indicated for use in Kaposi's sarcoma, ovarian cancer, and multiple myeloma with dose determined by square meters of body surface area.[12]

Hydrophilic drugs are typically loaded into liposomes by passive entrapment during liposome formation. Weakly basic amphipathic drugs are encapsulated using transmembrane gradients and trapping agents to load and stabilize the drug in the liposomal interior. The methods include transmembrane gradients of pH (formed using citric acid solutions), ammonium ions, transition metals, or drug solubility.[5]

Particle Formation and Radiolabeling

The steps in liposome formation have been described for many years: the process typically involves film hydration, sonication, and extrusion. Liposomes and micelles are the precursors of the microbubble's lipid monolayer shell. The lipids that form the shell of a typical microbubble or liposome are insoluble in water, with critical micelle concentrations well below micromolar values.

Steps involved in the microbubble shell assembly process include diffusion to the interface, aggregate disruption, and the subsequent hydrophobically driven adsorption, orientation, and lateral organization of the lipids into the monolayer film (Figure 2). Methods for creating lipid-coated microbubbles include mechanical disruption of the gas−liquid interface and injection of a gas stream that is induced to break up into a bubble train.[13] The different methods have their advantages and disadvantages. Mechanical disruption techniques such as sonication and amalgamation are readily available and economical and produce high yields (typically $\sim 10^9$ microbubbles per milliliter in a few seconds), but they create polydisperse size suspensions. Gas injection methods yield monodisperse sizes, but they are expensive and time-consuming to manufacture and generate much lower yields (typically $\sim 10^6$ microbubbles per milliliter over several hours).[13] Advances in both techniques are expected to improve the economy and quality of microbubble fabrication.

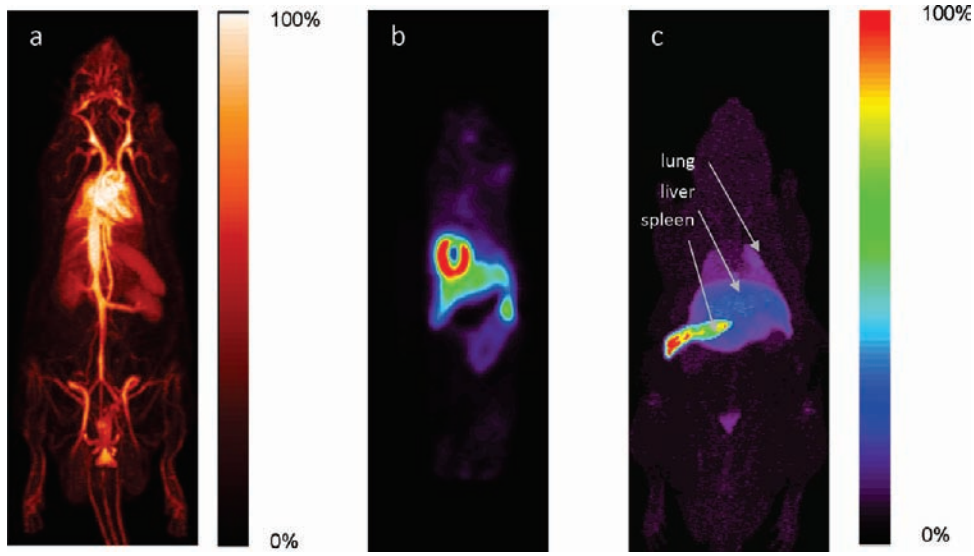

FIGURE 3. Positron emission tomography (PET) 90-min maximum intensity projection images of (a) long-circulating liposomes in a rat model, where the image is dominated by the blood pool, (b) short linear heart-targeted peptide (Cys-Arg-Pro-Pro-Arg) coated liposomes in a mouse model, where the image is dominated by the heart, and (c) microbubbles in a rat model, where the image is dominated by the spleen. Panels a and c are reproduced with permission from ref 16 (Copyright 2008 Elsevier), and panel b is reproduced with permission from ref 17 (Copyright 2008 Elsevier). Particles were radiolabeled by incorporating [^{18}F]FDP into the particle shell.

SCHEME 1. (a) Structure of [^{18}F]Fluorodipalmitin ([^{18}F]FDP) and (b) Integration of [^{18}F]FDP within particles

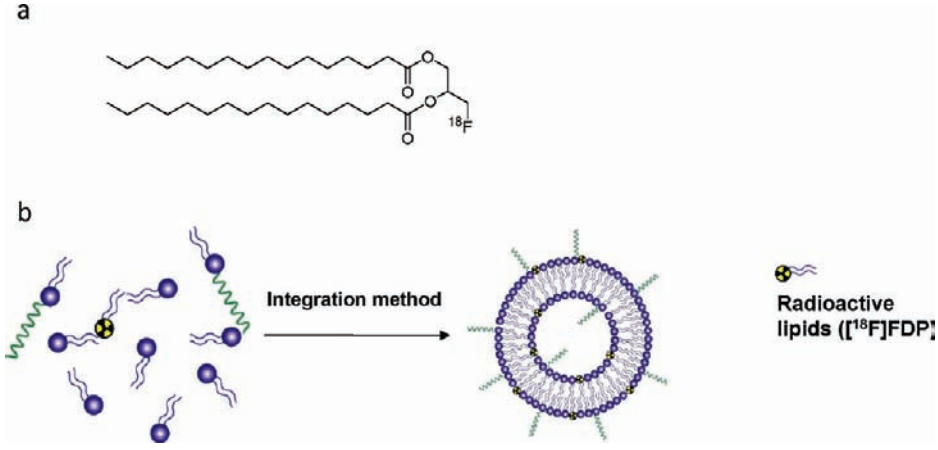

In order to assess and improve the stability and efficacy of these vehicles, we have explored the addition of radioisotopes to the lipid shell, including ^{18}F (half-life of 110 min) and ^{64}Cu (half-life of 12.7 h) isotopes for PET.[14] Our first methodology involved the attachment of ^{18}F to a dipalmitoyl lipid that was then incorporated within the liposome or microbubble (Scheme 1 and Figure 3). PET was then used to quantify the pharmacokinetics of both the circulating vehicle and individual lipid molecules. In order to facilitate radiolabeling of preformed and drug-loaded liposomes with ^{64}Cu, we have also attached 6-[*p*-(bromoacetamido)benzyl]-1,4,8,11-tetraazacyclotetradecane-*N*,*N*′,*N*″,*N*‴-tetraacetic acid, BAT[15] (Scheme 2). Here, the chelator is covalently bound to the lipid using solid phase synthesis, and ^{64}Cu is chelated in the final step.

PET chemistry facilitates tracking of the fate of injected microbubbles and liposomes, which exhibit vastly different pharmacokinetics.[16] Liposomes are long-circulating, resulting in a high-resolution PET image of the vascular structure, which was not thought to be feasible with PET (Figure 3a). With the addition of a vascular targeting ligand to the liposome shell, the accumulation of liposomes at the target can be very rapid. Using a short linear peptide targeted to heart endothelium, we have demonstrated that 40% of the injected dose of liposomes per gram of tissue can accumulate in the mouse heart within 100 s (Figure 3b),[17] although the receptor has not been identified. Ninety-minute maximum-intensity projections of radiolabeled microbubbles demonstrate rapid accumulation of the iso-

SCHEME 2. (a) Structure of BAT−PEG−lipid and (b) Integration of BAT−PEG−lipid within particles and radiolabeling with ^{64}Cu

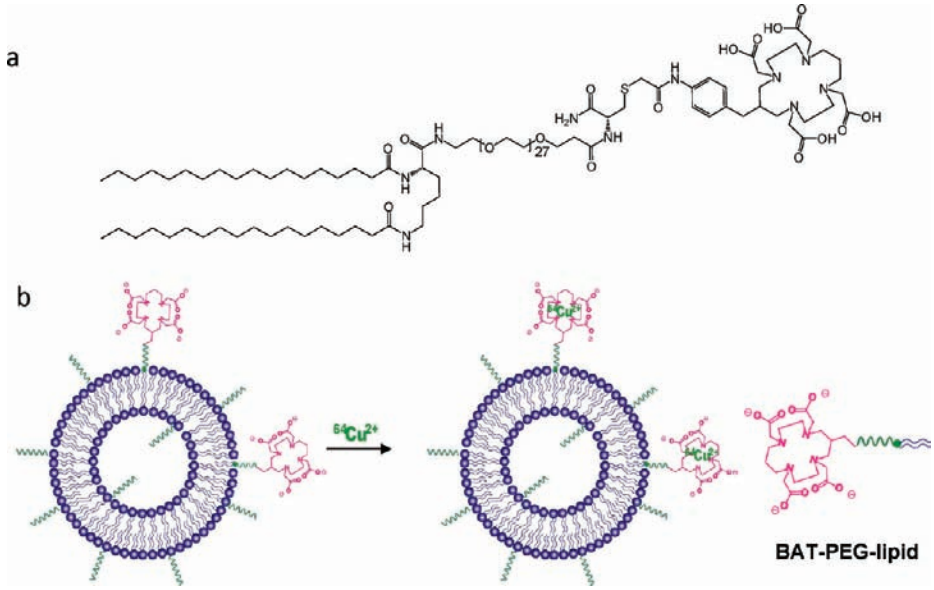

tope in the liver and spleen. Lipid-shelled microbubbles typically circulate for a period of minutes, with the shell accumulating in the liver and spleen and the gas core exhaled through the lungs (Figure 3c).[16] Using the ^{64}Cu methodology, liposomes can be tracked over multiple days, and targeting and activation by exogenous energy can be carefully studied.

Engineering for Stability and Persistence in Circulation

The lipid shell controls many of the properties relevant to medical applications. Fortuitously, the broad array of available lipid hydrophilic head groups and hydrophobic tail groups and the possibility of multicomponent mixtures offers a vast parameter space over which to manipulate the shell composition. For example, acyl chains of different lengths (Figure 1a) and degrees of saturation, charged headgroups, and steric stabilizers such as poly(ethylene glycol) (PEG) can be used. Longer acyl chains are used to increase lipid-shelled particle stability on the shelf and *in vivo*.[18] Saturated acyl chains are desired for their high degree of packing. The attractive forces arising from van der Waals and hydrophobic interactions between the lipid acyl chains increase with chain length. Lipids with longer acyl chains therefore make more cohesive membranes. For a given headgroup, acyl chain length dictates the phase state of the shell. Lipids above their main phase transition temperature (T_m) yield less ordered (expanded) phases, while those below their T_m organize into more ordered (solid) phases.

Microbubbles designed for medical applications typically comprise two main components: a matrix-forming phospholipid and an emulsifying lipid.[18] The emulsifying lipid usually contains a PEG group and is necessary for the efficient production of lipid-coated particles. PEG also provides a steric brush that minimizes lipid shell interactions with blood components. This is critical because particulate imaging systems may be recognized by opsonins or receptors present at cell surfaces and then removed via the reticuloendothelial system (RES) and features that facilitate avoidance of such recognitions are referred to as being "stealth". The time-averaged brush height and structure can be determined analytically from self-consistent field theory. Hindrance of protein diffusion to the surface is best achieved with the polymer chains in the brush configuration.[19] This is achieved when the intermolecular spacing is less than the polymer radius of gyration, such that lateral overlap interactions between the polymer chains force them to stretch outward. Ligands may be covalently attached to the distal end of PEG for targeting purposes.[18] There are limits to PEG grafting density and chain length. PEG chain lengths beyond 5 kDa make the emulsifier too hydrophilic, and the molecules do not incorporate well into liposomes or microbubbles. Grafting density is limited by lateral repulsive forces between the PEG chains that prevent tight packing of the acyl chains.[10,20] In microbubbles, for example, formulations become unstable with an emulsifier concentration above 20 mol% 2-kDa PEG.[21] On the other hand, short chains do not provide enough steric stabilization;

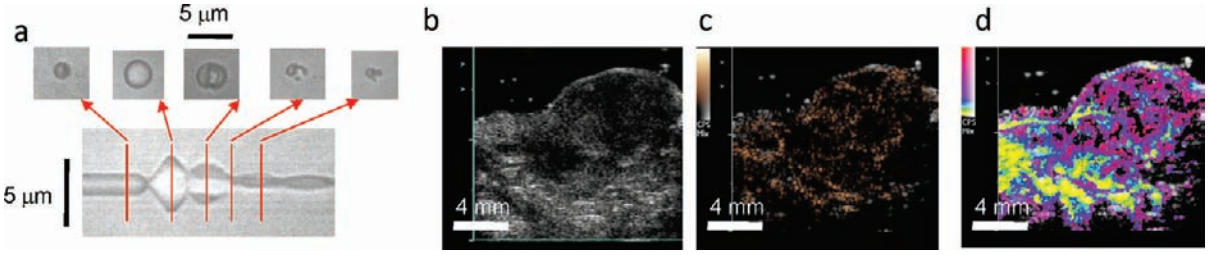

FIGURE 4. Insonation and imaging of microbubbles. (a) Image of a line through the center of a microbubble over time as the sound waves produce oscillations in microbubble diameter. Two-dimensional images of the microbubble are overlaid at the corresponding time points. (b) Gray scale ultrasound image of a tumor acquired at a center frequency of 14 MHz. (c) Corresponding image of microbubble density within the tumor created with Contrast Pulse Sequence (CPS) from Siemens Medical Solutions (MountainView CA). (d) Parametric map of the time required for microbubbles to fill each voxel after a high intensity pulse ruptures the bubbles, where color indicates time from 0.5 (yellow) to 10 s (pink). A 7-MHz pulse sequence consisting of low amplitude imaging pulses interleaved with high amplitude disruptive pulses was used to acquire the data. Such maps provide an assessment of local vascular functionality.

microbubbles formed using 1-kDa PEG were shown to coalesce to form macrobubbles within a few minutes.

From the preceding discussion, it is clear that the lipid shell is at least a binary mixture containing a phospholipid and emulsifier. While the two components were initially thought to be miscible within the monolayer shell of a microbubble, it is now recognized that they can demix to form domains.[21] Phase separation in the microbubble shell can be observed directly with fluorescence microscopy (Figure 2) and is similar to that of lung surfactant on a Langmuir trough, in which demixing of dipalmitoyl phosphatidylcholine (DPPC) into domains surrounded by a less ordered mixture of lipids and surfactant proteins has been observed.[22] Thus, while the species may be well mixed in liposomes, they can demix in the microbubble shell. Control over lipid shell microstructure is possible through crystallization of the domains by cooling after melting.[10,23] According to classical nucleation−growth theory, slow cooling through the phase transition favors growth, while rapid cooling favors nucleation. Defect density can also be increased through the use of longer acyl chains, which produce more dendritic and branched domains[23] (Figure 2).

Engineering for Ultrasound Imaging

The microbubble response to the driving pressure is also dependent on acyl chain length. Microbubbles coated with C_{12} lipids are highly unstable, while those coated with C_{24} are highly robust.[24] The high mechanical rigidity of phospholipid shells below their T_m was demonstrated by Needham and coworkers.[10] Our laboratory has extensively studied the response of microbubbles to ultrasound waves using both optical and acoustical techniques, as recently summarized in ref 25. These small gas bubbles expand and contract in response to each acoustic cycle. This oscillation creates a propagating wave that is detected by an ultrasound transducer to assess the relative concentration of bubbles in each region (Figure 4c). At moderate acoustic pressures, small amounts of gas are lost from the bubble with each cycle of expansion and contraction. The gas permeability of the lipid microbubble shell decreases exponentially with increasing acyl chain length when below the lipid T_m. Monolayer permeability also decreases exponentially with increasing collision area of the permeating gas. Based on this analysis, perfluorobutane is expected to permeate through the lipid shell at a rate approximately one thousand times slower than oxygen. Following each ultrasound pulse, excess lipid (beyond the maximum surface density) must collapse from the monolayer plane to accommodate the contracting surface of the shrinking gas core.[24] For shorter acyl chains, small lipid aggregates are ejected with each pulse (Figure 2). Using longer acyl chains, the more cohesive collapsed phase remains attached to the monolayer shell as the gas bubble decreases in diameter. When driven with a high pressure (~250 kPa or greater), microbubble fragmentation can occur, producing a set of small bubble fragments. The lipid shell reforms around the smaller bubble or bubble fragments and continues to serve as a barrier to passive diffusion (Figure 4a).

Microbubble oscillation and fragmentation are important for medical imaging and drug delivery. For example, imaging with lipid-shelled microbubbles can add information to conventional gray scale images of a tumor (Figure 4b). Specialized imaging pulse sequences are used to map microbubble density (Figure 4c). Microbubbles can be intentionally fragmented with a high amplitude pressure pulse, and the time required for each voxel to refill with microbubbles is quantified and indicated in color to yield a functional image of the tumor vasculature (Figure 4d).

SCHEME 3. Scheme Employed in Peptide–PEG–Lipid Conjugate Synthesis

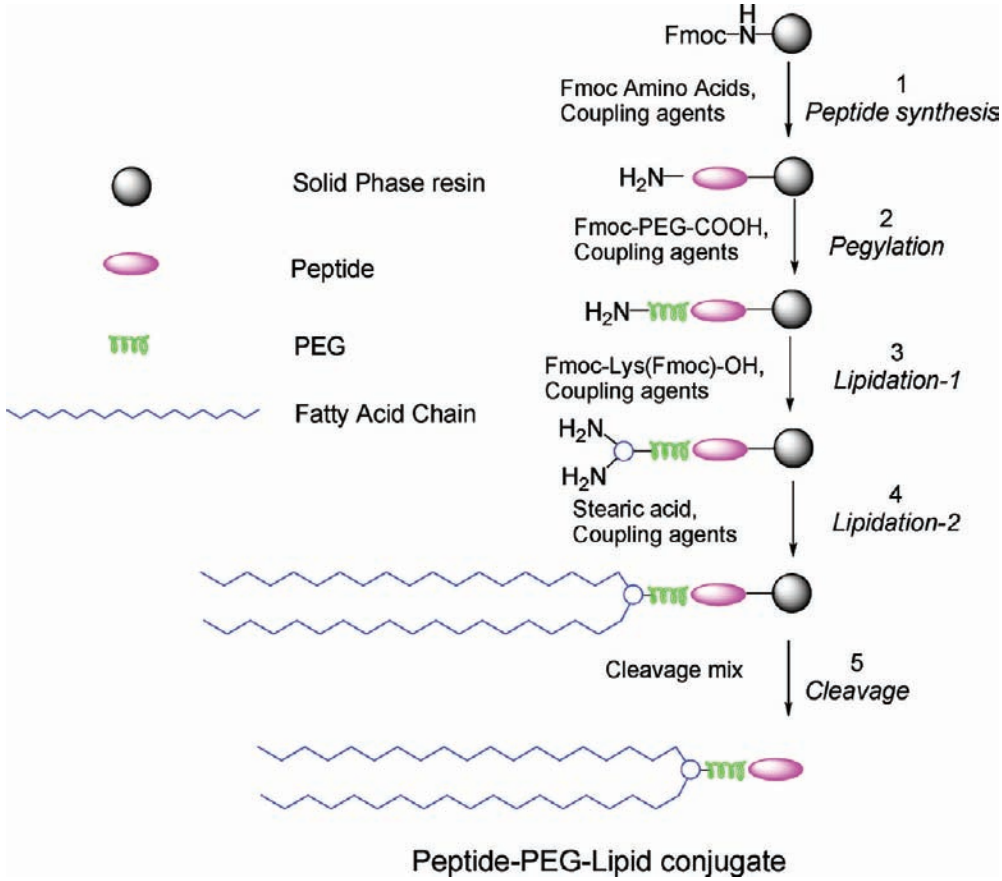

Engineering for Receptor Targeting and Membrane Fusion

Attachment of antibodies to preformed liposomes or microbubbles may be accomplished through the use of a common coupling chemistry, such as avidin–biotin, maleimide–thiol, or carboxylic acid–amine.[18] Alternatively, attachment of a small molecule ligand to a microbubble or liposome can be accomplished by coupling the ligand to the lipid prior to particle formation. In our laboratory, we have developed solid phase synthesis techniques for coupling ligands, poly(ethylene glycol) (PEG) and peptides (Scheme 3); we also employ this technique for coupling lipids and chelators.[15] First, Fmoc amino acids are coupled onto a solid phase resin to obtain peptides (step 1), and then Fmoc-PEG-COOH is coupled until the expected PEG length is reached (step 2). After the PEGylation step is finished, Fmoc-Lys(Fmoc)-OH and stearic acid are coupled in sequence (steps 3 and 4). Peptide–PEG–lipid conjugates are obtained after cleavage and purification through HPLC.

Images of targeted microbubbles are created by detecting the presence of bound bubbles as free microbubbles clear from the circulation[26] (Figure 5). Typically, at the time when most free bubbles have cleared, the bound microbubbles are destroyed by a high-intensity pulse, and the difference between the images before and after the destructive pulse is used to estimate the density of bound bubbles. Examples of postprocessed ultrasound images are shown in Figure 5a,b. Echistatin-targeted microbubbles showed more accumulation than control (not targeted) microbubbles within the fibroblast-growth-factor-stimulated Matrigel plug in a rat model.[27]

With a liposomal system, the targeting ligand must be exposed above the surrounding PEG brush layer in order for receptor–ligand targeting to occur. Alternatively, a ligand attached to a microbubble can be hidden from the surrounding medium by using a bimodal system with the ligand tether being shorter than the surrounding methyl-terminated chains.[28] See Figure 5c,d for a schematic cartoon of the buried-ligand architecture. The purpose of ligand concealment is to prevent binding to serum proteins and nonspecific adhesion. In particular, complement protein C3b has an unstable thioester group that binds to nucleophilic groups, such as hydroxyls or amines.[29] Such nucleophilic groups are almost always present on biological ligands. Nonspecific binding of C3b activates the complement cascade, stimulates inflamma-

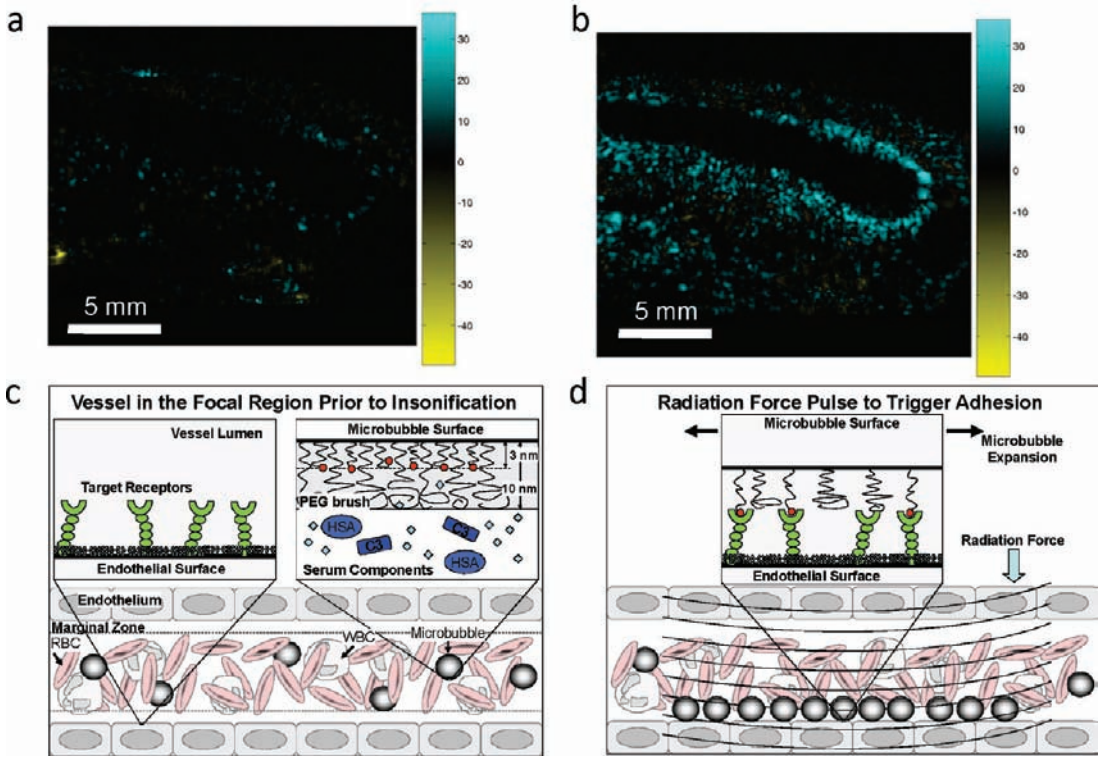

FIGURE 5. Vascular targeting: (a, b) Ultrasound images of microbubbles bound to angiogenic vasculature in a fibroblast-growth-factor-stimulated Matrigel plug where panel a is control microbubble and panel b is echistatin-targeted microbubble. (c) Prior to the application of ultrasound radiation force, microbubbles are uniformly distributed within the blood vessel. (d) After the application of radiation force, microbubbles are deflected to the vessel wall, resulting in enhanced targeting. Cartoons c and d are reproduced with permission from ref 28 (Copyright 2008 Elsevier).

tion, and tags the particle for removal by the RES. Clearly, this is to be avoided during systemic transit to the region of interest. Importantly, the ligand can be transiently revealed owing to surface area dilation and forward momentum of the microbubble center of mass during low-amplitude oscillations near the microbubble resonance frequency (i.e., radiation force). This allows temporally and spatially triggered binding and adhesion, which is unique to microbubbles. The use of radiation force promotes efficient adhesion of microbubbles with the buried-ligand architecture to receptor-bearing surfaces.[28] The ligand tether must be long and flexible enough so that the recoil force of the polymer chain does not detach the ligand from the receptor after the ultrasound pulse is finished and the shell has recovered the static brush structure.

Engineering for Drug Loading and Release

A large body of literature exists for liposome loading with drugs,[30] where larger diameter liposomes clearly have greater loading capacity. There is a trade-off, however, because liposomes with a diameter between 60 and 150 nm can exit through the leaky tumor endothelium,[31] while larger liposomes cannot. Classical temperature-sensitive liposomes have incorporated lipids with a short acyl chain, combining dipalmitoyl-phosphatidylcholine (DPPC) with small amounts of distearoyl-phosphatidylcholine (DSPC) to create a particle with a release rate that changes by a factor of 100 with heat.[4] Disadvantages of this specific approach include the relatively poor plasma stability and relatively high phase transition temperature. One strategy employed to hasten the release of a drug from a temperature-sensitive liposome and decrease the required temperature is the inclusion of a lysolipid fraction.[32] Such formulations have been shown to rapidly and efficiently release doxorubicin and cisplatin from temperature-sensitive liposomes; however, heat must be applied rapidly after injection.[33] Ongoing work in our laboratory involves the engineering of temperature-sensitive liposomes with enhanced stability. Our initial data with radiolabeled liposomes have demonstrated the opportunity to deliver as much as 19% injected dose per gram of tissue into tumor.

Effective loading and delivery with microbubble vehicles remains challenging because the loading of microbubbles is generally limited by the surface area. Layer-by-layer assembly has been proposed as a method to increase the drug loading of liposomes, nanoparticles,[34] and microbubbles (Figure 6a).[35] Successive layers of charged lipid are adsorbed on the shell surface, resulting in a 10-fold enhancement in the mass

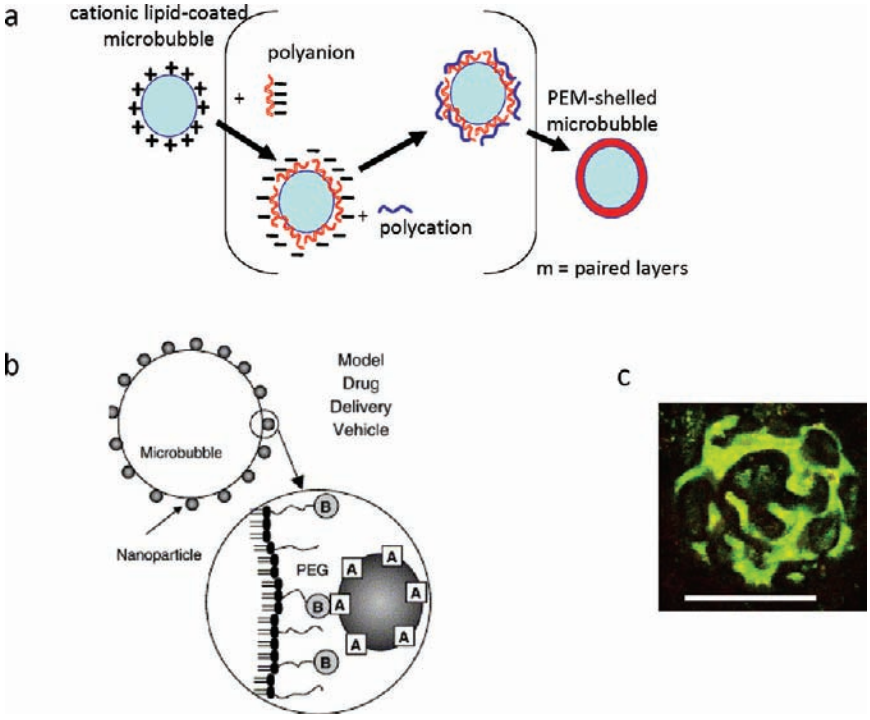

FIGURE 6. Enhancing drug and gene loading: (a) layer-by-layer loading of DNA on the surface of a particle; (b) hybrid vehicle composed of microbubbles and liposomes or nanoparticles; (c) confocal fluorescence image of a microbubble showing heterogeneous distribution and colocalization of DNA (red) and fluorescein-isothiocyanate−poly(L-lysine). Scale bar is 5 um. Panels a and c are reproduced with permission from ref 32 (Copyright 2000 American Association for Cancer Research); panel b is reproduced with permission from ref 38 (Copyright 2006 Elsevier).

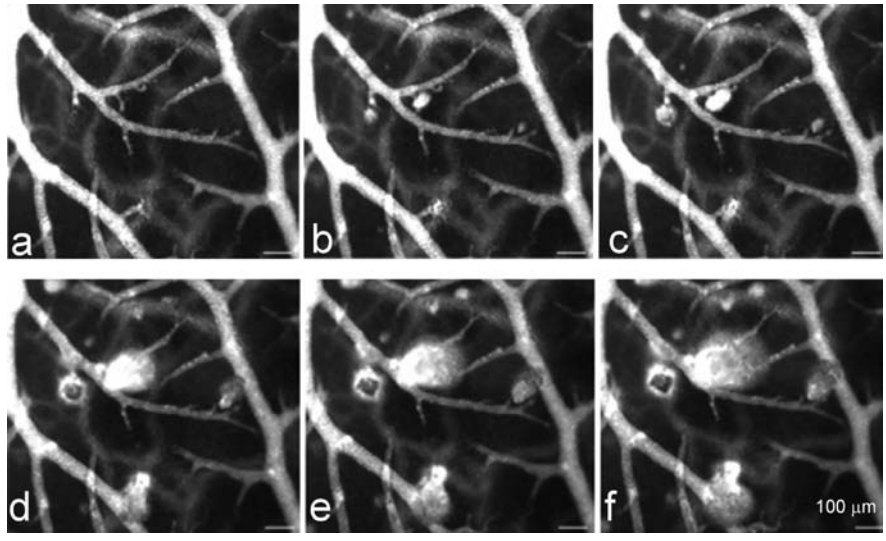

FIGURE 7. Enhanced drug and gene delivery achieved with the combination of particles and ultrasound. Insonation of circulating microbubbles in the chorioallantoic membrane model results in small vascular defects through which a fluorescent dye is transported. Reproduced with permission from ref 27 (Copyright 2007 Radiological Society of North America). Panels a−f are a sequence of images acquired from 1.00-MHz center frequency insonation at a peak negative pressure of 1.3 MPa. The panel a image was acquired before insonation; panels b−f images were acquired 0.06, 0.12, 1.24, 2.24, and 3.24 s after insonation began, respectively, demonstrating the transport of the fluorescent probe from the vasculature to the tissue interstitium.

of DNA adherent to the microbubble shell. Oils may be used to enhance loading, where the drug is solubilized within the oil.[36] The inclusion of paclitaxel within an oil coating has been shown to increase drug loading and facilitate the transfer of drugs from the microbubble shell to the endothelium during insonation.[37]

Drug loading of microbubbles can be greatly enhanced by the attachment of nanoparticles or liposomes on the

microbubble surface, where we find that thousands of small unilamellar liposomes can be attached to a single microbubble without significantly decreasing microbubble oscillation.[37] Loading of liposomes onto microbubbles offers a strategy to combine the unique characteristics of these two vehicles. We also find that the uneven surface of the hybrid vehicle facilitates the transport of lipids from the vehicle to the cell membrane (Figure 6b,c).[37] Further, the hybrid vehicles respond to the pressure wave and can easily be deflected to the vessel wall by a train of low-pressure ultrasound pulses (radiation forces).[38] The application of a pulse sequence designed to bring the microbubble into contact with the vessel wall and then fragment the microbubble has been shown to effectively deposit a targeted nanoparticle on the vessel wall.[38]

Optimizing the Biological Effects of Ultrasound with Vehicle Engineering

Therapeutic effects can be generated by microbubble oscillation in the ultrasound field, altering the permeability of endothelial cells and enhancing clot dissolution in applications including stroke and deep vein thrombosis.[39] Microbubbles are also being used to deliver genes, proteins, chemotherapeutics, and other compounds.[40] When driven by a sound wave, the wall of the microbubble reaches a velocity of hundreds to thousands of meters per second.[41] Physical phenomena associated with this oscillation have been shown to include liquid jet and shock wave formation; the microbubble diameter, microbubble concentration, vessel diameter, and ultrasound parameters are critical to defining the biological effect of the oscillating microbubble. Here, spatial localization of the effect is obtained primarily through positioning of the ultrasound focus. The ability to use ultrasound to image, push and break the microbubbles provides a unique level of external control over when and where a drug is released and its subsequent access to the extravascular space (Figure 7a).[27]

Furthermore, it has long been recognized that mild hyperthermia can increase vascular permeability and drug deposition.[7] The development of well-controlled commercial instrumentation linking ultrasound with magnetic resonance imaging has facilitated high-resolution mapping of temperature. Thus, the use of mild hyperthermia to induce changes in delivery vehicles is of renewed interest.

Conclusions and Future Directions

Microbubbles and liposomes may be used with ultrasound for diagnostic and therapeutic applications. Microbubbles are typically the choice for imaging, whereas both liposomes and microbubbles may be used for drug delivery. Whereas microbubbles are mechanically activated, liposomes are typically thermally activated. Many physicochemical properties depend on lipid composition, and therefore similar themes such as membrane cohesiveness, defect density, and PEG shielding apply to both systems. More work needs to be done to improve drug loading, retention in circulation, immunogenicity, and targeting efficiency. Future investigations likely will focus on the membrane physicochemical properties, the interactions with ultrasound, and the underlying mechanisms of the associated bioeffects.

We acknowledge the support of the NIH, Grants R01 CA103828 and CA112356.

BIOGRAPHICAL INFORMATION

Katherine Ferrara received her Ph.D. in Electrical Engineering from UC Davis in 1989. She held appointments at the Riverside Research Institute and the University of Virginia before her recruitment to UC Davis to found the Department of Biomedical Engineering. She is a fellow of the Acoustical Society of America, the American Institute of Medical and Biological Engineering, and the Biomedical Engineering Society.

Mark Borden received his Ph.D. in Chemical Engineering from UC Davis in 2003 and worked with Katherine Ferrara in Biomedical Engineering at UC Davis until 2007, when he became Assistant Professor of Chemical Engineering at Columbia University. He recently received the NYSTAR James D. Watson Investigator Award for his work on microbubbles.

Hua Zhang received her Ph.D from Polytechnic University in 2005 in Chemical Engineering. Since 2005, she has been working with Katherine Ferrara in Biomedical Engineering at UC Davis. Her research interests include targeted imaging and drug delivery.

FOOTNOTES

*To whom correspondence should be addressed. Telephone number: (530)754-9436. E-mail address: kwferrar@ucdavis.edu.

REFERENCES

1 Serfis, A. B.; Katzenberger, R.; Williams, K.; Tran, N. Association of blood clotting factors I and VII with phospholipid monolayers at the air-water interface. *J. Colloid Interface Sci.* **1999**, *215*, 356–363.

2 Morgan, K. E.; Allen, J. S.; Dayton, P. A.; Chomas, J. E.; Klibanov, A. L.; Ferrara, K. W. Experimental and theoretical evaluation of microbubble behavior: Effect of transmitted phase and bubble size. *IEEE Trans. Ultrason. Ferroelectr. Frequency Control* **2000**, *47*, 1494–1509.

3 Kaul, S. Myocardial contrast echocardiography: A 25-year retrospective. *Circulation* **2008**, *118*, 291–308.

4 Yatvin, M.; Weinstein, J. N.; Dennis, W. H.; Blumenthal, R. Design of liposomes for enhanced local release of drugs by hyperthermia. *Science* **1978**, *202*, 1290–1293.

5 Drummond, D.; Noble, C. O.; Hayes, M. E.; Park, J. W.; Kirpotin, D. B. Pharmacokinetics and in vivo drug release rates in liposomal nanocarrier development. *J. Pharm. Sci.* **2008**, *97*, 4696–4740.

6 Celsion Corporation. Clinical trials. http://www.celsion.com/trials.cfm.

7 Dromi, S.; Frenkel, V.; Luk, A.; Traughber, B.; Angstadt, M.; Bur, M.; Poff, J.; Xie, J. W.; Libutti, S. K.; Li, K. C. P.; Wood, B. J. Pulsed-high intensity focused ultrasound and low temperature sensitive liposomes for enhanced targeted drug delivery and antitumor effect. *Clin. Cancer Res.* **2007**, *13*, 2722–2727.

8 Ahmed, M.; Monsky, W. E.; Girnun, G.; Lukyanov, A.; D'Ippolito, G.; Kruskal, J. B.; Stuart, K. E.; Torchilin, V. P.; Goldberg, S. N. Radiofrequency thermal ablation sharply increases intratumoral liposomal doxorubicin accumulation and tumor coagulation. *Cancer Res.* **2003**, *63*, 6327–6333.

9 Zhu, M. A.; Bashir, A.; Ackerman, J. J.; Yablonskiy, D. A. Improved calibration technique for in vivo proton MRS thermometry for brain temperature measurement. *Magn. Reson. Med.* **2008**, *60*, 536–541.

10 Kim, D. H.; Costello, M. J.; Duncan, P. B.; Needham, D. Mechanical properties and microstructure of polycrystalline phospholipid monolayer shells: Novel solid microparticles. *Langmuir* **2003**, *19*, 8455–8466.

11 Dressaire, E.; Bee, R.; Bell, D. C.; Lips, A.; Stone, H. A. Interfacial polygonal nanopatterning of stable microbubbles. *Science* **2008**, *320*, 1198–1201.

12 http://www.doxil.com/common/prescribing_information/DOXIL/PDF/DOXIL_PI_Booklet.pdf.

13 Talu, E.; Hettiarachchi, K.; Powell, R. L.; Lee, A. P.; Dayton, P. A.; Longo, M. L. Maintaining monodispersity in a microbubble population formed by flow-focusing. *Langmuir* **2008**, *24*, 1745–1749.

14 Marik, J.; Tartis, M. S.; Zhang, H.; Fung, J. Y.; Kheirolomoom, A.; Sutcliffe, J. L.; Ferrara, K. W. Long-circulating liposomes radiolabeled with [F-18]fluorodipalmitin ([F-18]FDP). *Nucl. Med. Biol.* **2007**, *34*, 165–171.

15 Seo, J. W.; Zhang, H.; Kukis, D. L.; Meares, C. F.; Ferrara, K. W. A Novel method to label preformed liposomes with (CU)-C-64 for positron emission tomography (PET) imaging. *Bioconjugate Chem.* **2008**, *19*, 2577–2584.

16 Tartis, M. S.; Kruse, D. E.; Zheng, H.; Zhang, H.; Kheirolomoom, A.; Marik, J.; Ferrara, K. W. Dynamic microPET imaging of ultrasound contrast agents and lipid delivery. *J. Controlled Release* **2008**, *131*, 160–166.

17 Zhang, H.; Kusunose, J.; Kheirolomoom, A.; Seo, J. W.; Qi, J.; Watson, K.; Lindfors, H.; Ruoslahti, E; Sutcliffe, J. L.; Ferrara, K. W. Dynamic imaging of arginine-rich heart-targeted vehicles in a mouse model. *Biomaterials* **2008**, *29*, 1976–1988.

18 Klibanov, A. L. Ligand-carrying gas-filled microbubbles: Ultrasound contrast agents for targeted molecular imaging. *Bioconjugate Chem.* **2005**, *16*, 9–17.

19 Leckband, D.; Sheth, S.; Halperin, A. Grafted poly(ethylene oxide) brushes as nonfouling surface coatings. *J. Biomater. Sci.: Polym. Ed.* **1999**, *10*, 1125–1147.

20 Duncan, P. B.; Needham, D. Test of the Epstein-Plesset model for gas microparticle dissolution in aqueous media: Effect of surface tension and gas undersaturation in solution. *Langmuir* **2004**, *20*, 2567–2578.

21 Borden, M. A.; Martinez, G. V.; Ricker, J.; Tsvetkova, N.; Longo, M.; Gillies, R. J.; Dayton, P. A.; Ferrara, K. W. Lateral phase separation in lipid-coated microbubbles. *Langmuir* **2006**, *22*, 4291–4297.

22 Discher, B. M.; Maloney, K. M.; Schief, W. R.; Grainger, D. W.; Vogel, V.; Hall, S. B. Lateral phase separation in interfacial films of pulmonary surfactant. *Biophys. J.* **1996**, *71*, 2583–2590.

23 Borden, M. A.; Pu, G.; Runner, G. J.; Longo, M. L. Surface phase behavior and microstructure of lipid/PEG-emulsifier monolayer-coated microbubbles. *Colloids Surf. B* **2004**, *35*, 209–223.

24 Borden, M. A.; Kruse, D. E.; Caskey, C. F.; Zhao, S. K.; Dayton, P. A.; Ferrara, K. W. Influence of lipid shell physicochemical properties on ultrasound-induced microbubble destruction. *IEEE Trans. Ultrason. Ferroelectr. Frequency Control* **2005**, *52*, 1992–2002.

25 Qin, S.; Caskey, C. F; Ferrara, K. W. Ultrasound contrast microbubbles in imaging and therapy: physical principles and engineering. *Phys. Med. Biol.* **2009**, Mar 21; 54(6):R27−57. Epub 2009 Feb 19.

26 Stieger, S. M.; Dayton, P. A.; Borden, M. A.; Caskey, C. F.; Griffey, S. M.; Wisner, E. R.; Ferrara, K. W. Imaging of angiogenesis using Cadence (TM) contrast pulse sequencing and targeted contrast agents. *Contrast Media Mol. Imaging* **2008**, *3*, 9–18.

27 Stieger, S. M.; Caskey, C. F.; Adamson, R. H.; Qin, S.; Curry, F. R.; Wisner, E. R.; Ferrara, K. W. Enhancement of vascular permeability with low-frequency contrast-enhanced ultrasound in the chorioallantoic membrane model. *Radiology* **2007**, *243*, 112–121.

28 Borden, M. A.; Zhang, H.; Gillies, R. J.; Dayton, P. A.; Ferrara, K. W. A stimulus-responsive contrast agent for ultrasound molecular imaging. *Biomaterials* **2008**, *29*, 597–606.

29 Janssen, B. J. C.; Huizinga, E. G.; Raaijmakers, H. C. A.; Roos, A.; Daha, M. R.; Nilsson-Ekdahl, K.; Nilsson, B.; Gros, P. Structures of complement component C3 provide insights into the function and evolution of immunity. *Nature* **2005**, *437*, 505–511.

30 Torchilin, V. P. Targeted pharmaceutical nanocarriers for cancer therapy and Imaging. *AAPS J.* **2007**, *9*, E128–E147.

31 Sapra, P.; Allen, T. M. Ligand-targeted liposomal anticancer drugs. *Prog. Lipid Res.* **2003**, *42*, 439–462.

32 Needham, D.; Anyarambhatla, G.; Kong, G.; Dewhirst, M. W. A new temperature-sensitive liposome for use with mild hyperthermia: Characterization and testing in a human tumor xenograft model. *Cancer Res.* **2000**, *60*, 1197–1201.

33 Woo, J.; Chiu, G. N. C.; Karlsson, G.; Wasan, E.; Ickenstein, L.; Edwards, K.; Bally, M. B. Use of a passive equilibration methodology to encapsulate cisplatin into preformed thermo sensitive liposomes. *Int. J. Pharm.* **2008**, *349*, 38–46.

34 Haidar, Z. S.; Hamdy, R. C.; Tabrizian, M. Protein release kinetics for core-shell hybrid nanoparticles based on the layer-by-layer assembly of alginate and chitosan on liposomes. *Biomaterials* **2008**, *29*, 1207–1215.

35 Borden, M. A.; Caskey, C. F.; Little, E.; Gillies, R. J.; Ferrara, K. W. DNA and polylysine adsorption and multilayer construction onto cationic lipid-coated microbubbles. *Langmuir* **2007**, *23*, 9401–9408.

36 Tartis, M. S.; McCallan, J.; Lum, A. F.; Labell, R.; Stieger, S. M.; Matsunaga, T. O.; Ferrara, K. W. Therapeutic effects of paclitaxel-containing ultrasound contrast agents. *Ultrasound Med. Biol.* **2006**, *32*, 1771–1780.

37 Kheirolomoom, A.; Dayton, P. A.; Lum, A. F. H.; Little, E.; Paoli, E. E.; Zheng, H.; Ferrara, K. W. Acoustically-active microbubbles conjugated to liposomes: Characterization of a proposed drug delivery vehicle. *J. Controlled Release* **2007**, *118*, 275–284.

38 Lum, A. F. H.; Borden, M. A.; Dayton, P. A.; Kruse, D. E.; Simon, S. I.; Ferrara, K. W. Ultrasound radiation force enables targeted deposition of model drug carriers loaded on microbubbles. *J. Controlled Release* **2006**, *111*, 128–134.

39 Holland, C. K.; Vaidya, S. S.; Datta, S.; Coussios, C. C.; Shaw, G. J. Ultrasound-enhanced tissue plasminogen activator thrombolysis in an in vitro porcine clot model. *Thromb. Res.* **2008**, *121*, 663–673.

40 Bekeredjian, R.; Chen, S. Y.; Frenkel, P. A.; Grayburn, P. A.; Shohet, R. V. Ultrasound-targeted microbubble destruction can repeatedly direct highly specific plasmid expression to the heart. *Circulation* **2003**, *108*, 1022–1026.

41 Chomas, J. E.; Dayton, P. A.; May, D.; Allen, J.; Klibanov, A.; Ferrara, K. Optical observation of contrast agent destruction. *Appl. Phys. Lett.* **2000**, *77*, 1056–1058.